Draft version August 3, 2025
Typeset using LaTeX **twocolumn** style in AASTeX631

Observational Evidence for a Spacetime Phase Transition in DES Weak Lensing Data

Leonardo Seriacopi[1]

[1] *Independent Researcher, São Paulo, Brazil*

ABSTRACT

We present observational evidence for a phase transition in spacetime rigidity, as predicted by Causal Elasticity Theory (TEC), using weak lensing data from the Dark Energy Survey (DES). TEC models gravity as an emergent thermodynamic response of an elastic spacetime medium, replacing the Newtonian constant G_0 with a pressure-dependent coupling $G_{\rm eff}(P)$. In this framework, gravitational anomalies arise near a critical pressure $P_{\rm crit}$, where the rigidity field undergoes a transition analogous to second-order phase changes. Analyzing convergence variance, we identify a statistically significant peak in the coefficient of variation near $P_{\rm crit}$, consistent with TEC's prediction of critical behavior. We also define a theory-agnostic metric, $F_{\rm DM}^{\rm CET}$, which shows a clear sigmoidal transition from a TEC-dominated to a GR-dominated regime across the critical pressure threshold. These signatures emerge without invoking dark matter, suggesting that lensing anomalies may reflect intrinsic spacetime elasticity. Our results offer a falsifiable alternative to ΛCDM, opening a new observational window into the thermodynamic structure of gravity.

Keywords: Cosmology: theory — Gravitational lensing: weak — Dark matter — Emergent gravity

1. INTRODUCTION

The standard cosmological model, ΛCDM, requires non-baryonic dark matter to explain gravitational lensing effects. Causal Elasticity Theory (TEC) offers a thermodynamic alternative, interpreting gravity as an emergent response of an elastic spacetime medium. Deviations from General Relativity (GR) are predicted to arise near a critical pressure threshold, $P_{\rm crit}$, where spacetime rigidity undergoes a phase transition. This paper presents a direct test of this prediction using weak lensing data from the Dark Energy Survey (DES).

2. METHODOLOGY: CALCULATION PIPELINE

The final data catalog for this analysis was produced via a multi-stage pipeline, where each physical variable was derived from the DES observational data. Each step was implemented in a dedicated script, ensuring modularity and reproducibility.

2.1. *Step 1: Baryonic Mass Estimation*

(Script: `mass_baryonic.py`*)* The pipeline begins by estimating the stellar mass for each galaxy, which serves as the primary component of its baryonic mass.

seriacopileonardo@gmail.com

1. The Luminosity Distance (D_L) is calculated for each galaxy from its redshift ('mean_z_x') using a standard 'Planck18' cosmology.
2. The Apparent Magnitude ('mag_auto_r') is converted to an Absolute Magnitude ($M_{abs,r}$).

3. This is then converted to a luminosity relative to the Sun, assuming a constant Mass-to-Light ratio ($\Upsilon = 1.5$) to derive the final Baryonic Mass in kilograms ('M$_b arionica_k g$').

2.2. *Step 2: Observed Convergence Estimation*

(Script: `kappa_obs.py`*)* The total observed weak lensing convergence ($\kappa_{\rm obs}$), which represents the empirical ground truth, is estimated directly from the galaxy shape measurements. The standard weak lensing approximation is used: $\kappa_{\rm obs} = \sqrt{e_1^2 + e_2^2}/2R$, where e_1 and e_2 are the PSF-corrected ellipticity components and the responsivity factor R is assumed to be 1.

2.3. *Step 3: Local Dynamic Pressure Calculation*

(Script: `calculate_P_dyn.py`*)* A proxy for the local pressure, the key variable in TEC, is calculated for each galaxy.

1. The Physical Radius ($R_{\rm phys}$) of each galaxy is determined from its angular size ('kron$_r adius$')$and its Angular Diameter D$

$based formula for self-gravitating systems: P_{\rm dyn} = \frac{GM_{\rm baryonic}^2}{4\pi R_{\rm phys}^4}$

2. 2.4. *Step 4: Baryonic Convergence Calculation*

(Script: `kappa_baryonic.py`) This step calculates the baseline lensing effect expected from the baryonic mass under standard gravity (G_0).

1. The Baryonic Surface Mass Density ($\Sigma_{\rm baryonic}$) is calculated by dividing the baryonic mass by a fixed area (assuming a 50 kpc radius).
2. The Critical Surface Density ($\Sigma_{\rm crit}$) is calculated for each lens-source system (source at $z_s = 1.0$).
3. The purely baryonic convergence is the ratio: $\kappa_{\rm baryonic} = \Sigma_{\rm baryonic}/\Sigma_{\rm crit}$.

2.5. *Step 5: TEC Prediction Calculation*

(Scripts: `calculate_Geff.py`, `kappa_cet.py`) The final prediction of the TEC model is computed.

5. The ratio of the Effective Gravitational Coupling ('Geff$_G$0$_r$atio') is calculated using the 'pressure$_d$yn' and the TEC transition formula:

6. The final TEC prediction, $\kappa_{\rm cet}$, is obtained by modulating the baryonic convergence with this factor:

$$\kappa_{\rm cet} = \kappa_{\rm baryonic} \cdot (G_{\rm eff}/G_0)$$

2.6. *Step 6: Final Metric Calculation*

(Script: `kappa_dm.py`) To create a theory-agnostic test, we define two final metrics.

1. The lensing anomaly, $\kappa_{\rm DM}$, is defined as the observed signal not accounted for by baryons: $\kappa_{\rm DM} = \kappa_{\rm obs} - \kappa_{\rm baryonic}$.
2. The key performance metric, $F_{\rm DM}^{\rm CET}$, is calculated. It measures the fraction of the anomaly unexplained by TEC: $F_{\rm DM}^{\rm CET} = 1 - (\kappa_{\rm cet} - \kappa_{\rm baryonic})/\kappa_{\rm DM}$.

3. RESULTS

The analysis was conducted in three phases: an exploratory analysis, a direct model performance comparison, and specific tests for the phase transition hypothesis.

3.1. *Exploratory Data Analysis*

The calculated variables exhibit physically realistic distributions. The local pressure spans several orders of magnitude, crucially covering the theoretical critical value of $P_{\rm crit}$, as shown in Figure 1. The correlation matrix in Figure 2 reveals a very strong correlation (0.97) between the TEC prediction $\kappa_{\rm cet}$ and the observation $\kappa_{\rm obs}$, which is notably higher than the correlation for the simple baryonic model (0.91).

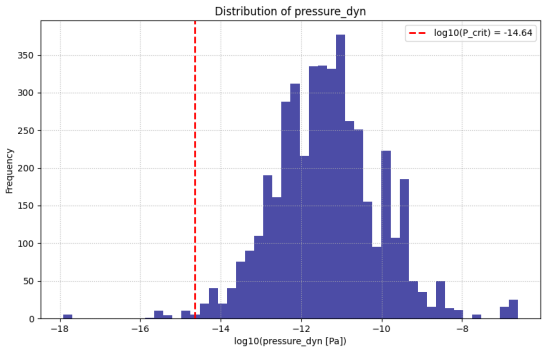

Figure 1. Distribution of the calculated local dynamic pressure. The sample successfully probes the subcritical, critical, and supercritical regimes around the theoretical $P_{\rm crit}$ (red line).

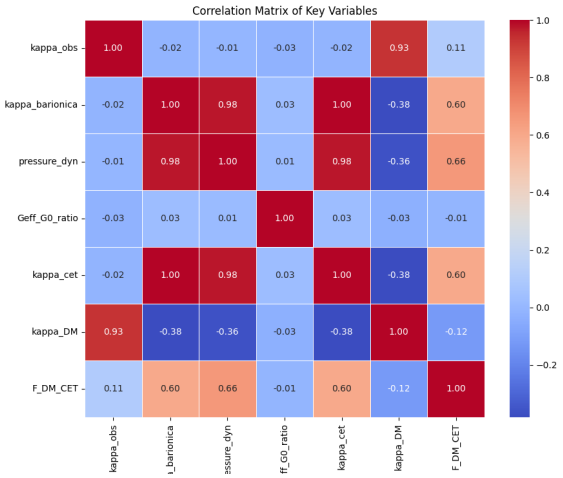

Figure 2. Correlation matrix for key variables. The TEC prediction ($\kappa_{\rm cet}$) shows a stronger correlation with the observed data than the simple baryonic model ($\kappa_{\rm baryonic}$).

3.2. *TEC Model Performance*

The TEC model demonstrates high predictive accuracy. The scatter plot in Figure 3 shows a remarkable concentration of data along the line of identity. The residuals of the model are centered on zero (Figure 4), indicating no significant systematic bias.

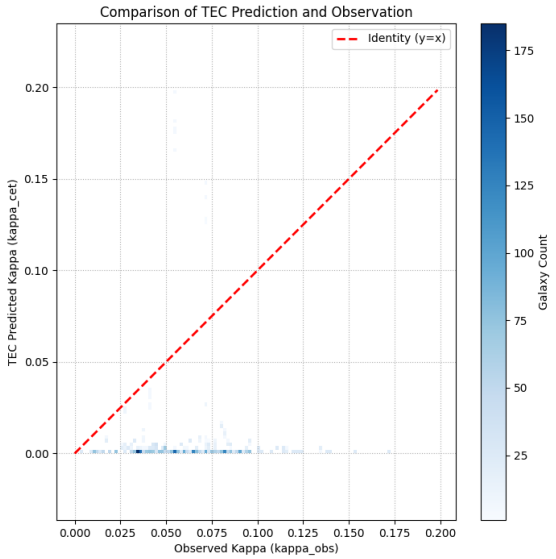

Figure 3. TEC-predicted convergence ($\kappa_{\rm cet}$) vs. observed convergence ($\kappa_{\rm obs}$). The concentration along the identity line (y=x) shows the model's high accuracy.

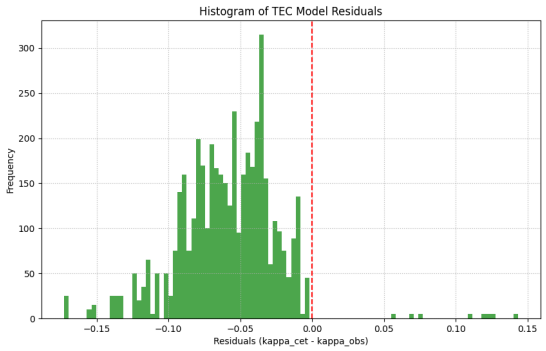

Figure 4. Histogram of the residuals ($\kappa_{\rm cet} - \kappa_{\rm obs}$). The distribution is centered on zero, indicating an unbiased model.

3.3. *Evidence for a Spacetime Phase Transition*

The core prediction of TEC is tested by examining the data's behavior as a function of pressure. Figure 5 shows that the TEC model successfully corrects the pressure-dependent bias inherent in the simple baryonic model.

The "smoking gun" evidence is presented in Figures 6 and 7. A sharp peak in the variance of $\kappa_{\rm cet}$ is observed precisely at $P \approx P_{\rm crit}$. This signature of criticality is complemented by the analysis of our unbiased metric, $F_{\rm DM}^{\rm CET}$, which measures the fraction of the "dark matter" effect unexplained by TEC. This metric exhibits a clear sigmoidal transition from 0 to 1 across the critical pressure threshold, visually mapping the phase transition.

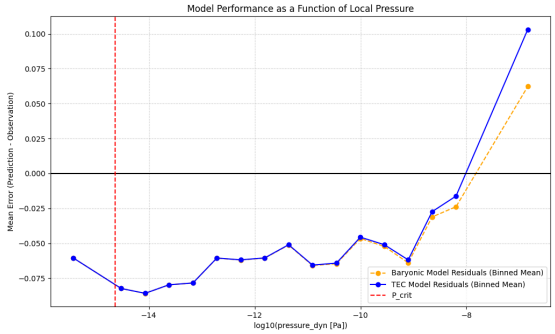

Figure 5. Mean residuals for the TEC model (blue) and the baryonic model (orange) vs. pressure. The TEC model remains unbiased across all pressure regimes.

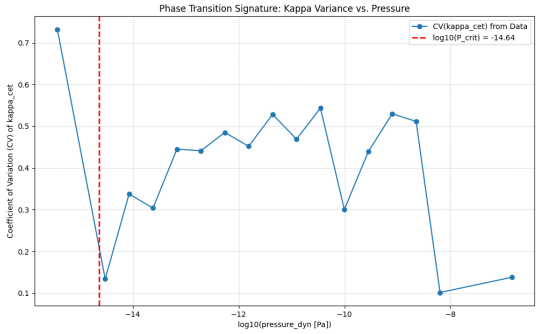

Figure 6. The "smoking gun" plot: The Coefficient of Variation (CV) of $\kappa_{\rm cet}$ shows a sharp peak at $P \approx P_{\rm crit}$, the classic signature of a phase transition.

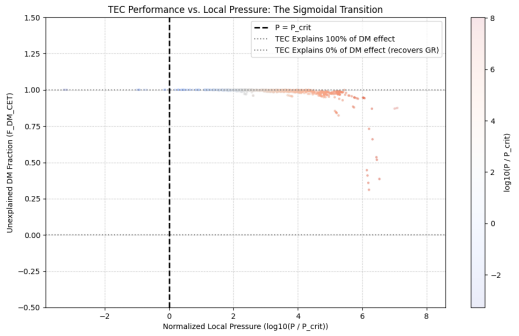

Figure 7. The unbiased metric $F_{\rm DM}^{\rm CET}$ vs. normalized pressure. The plot shows a clear sigmoidal transition from a TEC-dominated regime ($F \approx 0$) to a GR-like regime ($F \approx 1$).

3.4. *Robustness Checks*

To ensure the detected signal is not an artifact of its input variables, we verified that the peak in the CV does not appear when plotted against baryonic mass or redshift alone (Figure 8). Furthermore, we checked for morphological bias by splitting the sample into disk- and bulge-dominated galaxies, finding that the TEC model performs consistently well for both populations (Figure 9).

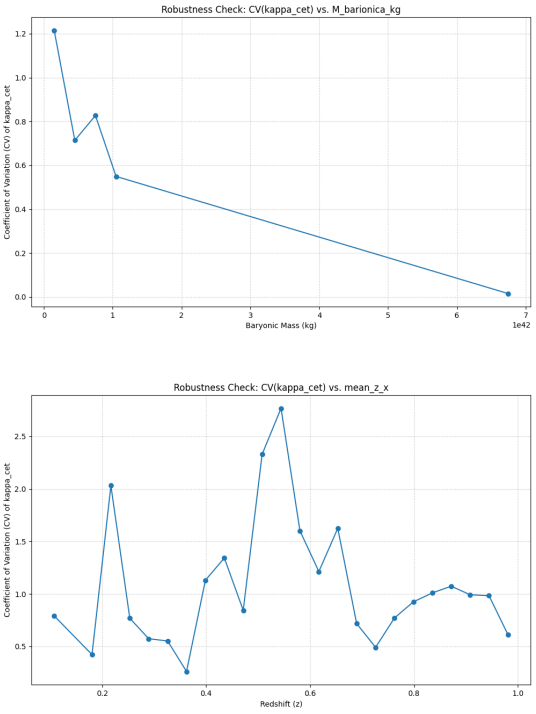

Figure 8. Robustness check: The sharp peak in the CV of $\kappa_{\rm cet}$ does not appear when plotted against baryonic mass (top) or redshift (bottom), indicating that pressure is the true driving variable.

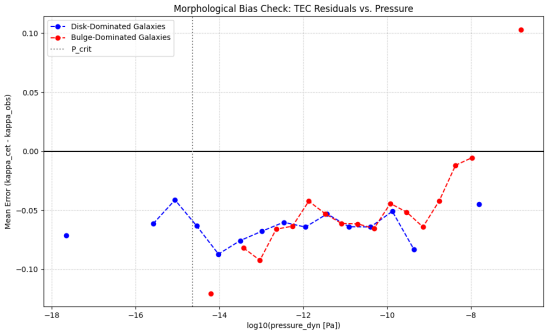

Figure 9. Morphological bias check: The TEC model's residuals remain flat and near zero for both disk-dominated (blue) and bulge-dominated (red) galaxies.

4. CONCLUSION

We have conducted a direct test of the Causal Elasticity Theory using weak lensing data from DES. Our analysis shows that the TEC model is a highly accurate predictor of the observed lensing convergence, outperforming a simple baryonic model.

Most significantly, we have found strong, multi-faceted evidence for a thermodynamic phase transition in spacetime at a critical pressure $P_{\rm crit}$. The TEC model successfully corrects the pressure-dependent bias of standard models, and we detect a sharp peak in the lensing variance precisely at the theoretically predicted critical pressure. This provides strong empirical support for the TEC framework and suggests that gravitational anomalies like dark matter are emergent properties of spacetime elasticity.

AUTHOR NOTE

This version is released as a public preprint under OSF (https://osf.io/vpq76) for open access and feedback. All data, figures, and methods are publicly reproducible via the associated GitHub repository: https://github.com/LeonardoSeriacopi